Short Communication

Genomic RNA sequence of *Feline coronavirus* strain FIPV WSU-79/1146

Charlotte Dye and Stuart G. Siddell

Division of Virology, Department of Pathology and Microbiology, School of Medical Sciences, University of Bristol, Bristol BS8 1TD, UK

Correspondence
Charlotte Dye
C.Dye@bristol.ac.uk

A consensus sequence of the *Feline coronavirus* (FCoV) (strain FIPV WSU-79/1146) genome was determined from overlapping cDNA fragments produced by RT-PCR amplification of viral RNA. The genome was found to be 29 125 nt in length, excluding the poly(A) tail. Analysis of the sequence identified conserved open reading frames and revealed an overall genome organization similar to that of other coronaviruses. The genomic RNA was analysed for putative *cis*-acting elements and the pattern of subgenomic mRNA synthesis was analysed by Northern blotting. Comparative sequence analysis of the predicted FCoV proteins identified 16 replicase proteins (nsp1–nsp16) and four structural proteins (spike, membrane, envelope and nucleocapsid). Two mRNAs encoding putative accessory proteins were also detected. Phylogenetic analyses confirmed that FIPV WSU-79/1146 belongs to the coronavirus subgroup G1-1. These results confirm and extend previous findings from partial sequence analysis of FCoV genomes.

Coronaviruses are enveloped, positive-strand RNA viruses that are associated mainly with enteric or respiratory diseases in humans, companion animals and livestock. Coronavirus particles contain a genomic RNA of approximately 27 000–30 000 nt and four structural proteins: namely, the spike glycoprotein S, the membrane protein M, the envelope protein E and the nucleocapsid protein N (Siddell *et al.*, 2005). In the infected cell, coronavirus gene expression starts with the translation of the replicase gene. The replicase gene comprises two large open reading frames (ORFs), designated ORF1a and ORF1b. The upstream ORF1a encodes a polyprotein of approximately 450–500 kDa, termed polyprotein pp1a, whereas ORF1a and ORF1b together encode a polyprotein of 750–800 kDa, termed polyprotein pp1ab (Siddell *et al.*, 2005). The pp1ab polyprotein is synthesized by a (−1) ribosomal frameshift during translation of the genomic RNA (Brierley, 1995; Thiel *et al.*, 2003). The polyproteins pp1a and pp1ab are then processed by virus-encoded proteinases to generate 15–16 end products [replicase or non-structural proteins (nsp)] and an unknown number of intermediate products (Ziebuhr *et al.*, 2000). The replicase proteins assemble to form the membrane-bound replication–transcription complex in the cytoplasm of the infected cell (Gosert *et al.*, 2002; Prentice *et al.*, 2004).

The coronavirus replication–transcription complex mediates replication of the genomic RNA and transcription of multiple subgenomic mRNAs. Coronavirus transcription is a complex process involving the discontinuous synthesis of up to eight (−)-strand RNAs of subgenomic size, which contain sequences corresponding to the 5′ and 3′ ends of the genome and serve as templates for the synthesis of subgenomic mRNAs (Sawicki & Sawicki, 1990; Spaan *et al.*, 1983). Important elements in the transcription process are the 'transcription-regulatory sequence elements' (TRS elements), which determine the fusion sites of leader and body-derived sequences of the subgenomic RNAs. The number of TRS elements correlates with the number of subgenomic mRNAs produced by a particular coronavirus. The subgenomic mRNAs express both structural and accessory proteins.

Feline coronavirus (FCoV) infection is extremely common in cats, and especially in kittens. For example, in the UK, approximately 40 % of the domestic cat population has been infected. In multi-cat households, this figure increases to about 90 % (Addie, 2000; Addie & Jarrett, 1992; Sparkes *et al.*, 1992). Natural infections with FCoV are usually transient, although a significant percentage of infections may become persistent (Addie & Jarrett, 2001). Infections may be asymptomatic or may result in mild, self-limiting gastrointestinal disease. In these cases, the causative agent is known as feline enteric coronavirus (FECV). In a small percentage of animals, a fatal, multisystemic, immune-mediated disease occurs and this is known as feline infectious peritonitis (FIP) (Pedersen, 1995). The virus associated with FIP is referred to as feline infectious peritonitis virus (FIPV). It is proposed that cats acquire FIPV by mutation of an endogenous FECV (Poland *et al.*, 1996; Vennema *et al.*, 1998) or, rarely, through excreted virus

from other FIPV-infected animals (Watt *et al.*, 1993). Any genetic difference(s) between FECV and FIPV that can account for their different pathogenicity remain to be identified.

FIPV WSU-79/1146 (P100) was obtained from the ATCC (VR-2202). The virus was plaque-purified and propagated in Crandell–Reese feline kidney (CrFK) cells, and viral poly(A)-containing RNA was isolated from infected cells by using TRIzol reagent and Dynabeads oligo (dT)$_{25}$ (Thiel *et al.*, 1997). Published sequence data for FIPV WSU-79/1146 (GenBank accession no. AY204704) and other FCoV strains (Herrewegh *et al.*, 1998) were used to design primers to amplify and sequence overlapping PCR products spanning the whole genome length (see Supplementary Table S1, available in JGV Online).

The genomic sequence of FCoV strain FIPV WSU-79/1146 comprises 29 125 nt, excluding the 3′ poly(A) tail. The sequence has been deposited in GenBank (accession no. DQ010921). The 5′ untranslated region (UTR) comprises 311 nt and includes an ORF of four codons (nt 117–128) that lies within a putative stem–loop structure [nt 102–140; see Supplementary Fig. S1(a), available in JGV Online] that is similar to the stem–loop III structure that has been identified as a *cis*-acting element in bovine coronavirus (BCoV) defective interfering RNA replication (Raman *et al.*, 2003). Also within this region, it is possible to identify another putative secondary structure, the so-called 'leader–TRS hairpin' or LTH [nt 65–128; Supplementary Fig. S1(b)] (Van Den Born *et al.*, 2004). The LTH structure encompasses the sequence 5′-CUAAAC-3′ (nt 93–98), which represents the core of the FIPV TRS element (de Groot *et al.*, 1988) and defines the fusion sites of leader and 'body'-derived sequences in coronavirus subgenomic mRNAs. The 3′ UTR of FIPV WSU-79/1146 would also be expected to contain *cis*-acting sequences and structural elements involved in viral RNA replication. In our analysis, we were able to identify two putative structures, spanning nt 28842–28964 (see Supplementary Fig. S2, available in JGV Online), that bear striking resemblance to the bulged stem–loop–pseudoknot structures identified by Masters and colleagues for MHV-A59 (Goebel *et al.*, 2004).

Analysis of the FIPV WSU-79/1146 genomic sequence with the NCBI graphical analysis tool ORF Finder identifies six ORFs that can be deduced to encode the non-structural and structural proteins of the virus (see Supplementary Table S2, available in JGV Online). ORF1a (nt 312–12208) and ORF1b (nt 12164–20209) encode the non-structural proteins. These ORFs overlap by 46 nt and a typical coronavirus 'slip site', 5′-UUUAAAC-3′ (nt 12173–12179), is located within this overlap. Adjacent and downstream of the 'slip site' is a putative 'pseudoknot' structure (see Supplementary Fig. S3, available in JGV Online). The 'slip site' and 'pseudoknot' are elements required for programmed (−1) ribosomal frameshifting during translation of the coronavirus genomic RNA (Brierley, 1995). In the case of FIPV WSU-79/1146, this results in the expression of

two primary translation products, pp1a and pp1ab, that are predicted to have molecular masses of 441·3 and 742·7 kDa, respectively. The ORFs encoding structural proteins are ORF S (nt 20206–24564), ORF E (nt 25722–25970), ORF M (nt 25981–26769) and ORF N (nt 26782–27915). The predicted translation products are the spike glycoprotein (160 kDa), the envelope protein (9·4 kDa), the membrane protein (29·8 kDa) and the nucleocapsid protein (42·7 kDa), respectively. Phylogenetic analysis shows that the FIPV WSU-79/1146 non-structural and structural proteins are related closely to their *Transmissible gastroenteritis virus* (TGEV) homologues, less closely to their *Human coronavirus 229E* (HCoV-229E) homologues and most distantly to their *Murine hepatitis virus* (MHV) and *Infectious bronchitis virus* (IBV) homologues. These data are consistent with the accepted phylogeny of coronaviruses that places FCoV in subgroup G1-1 of coronavirus group 1 (González *et al.*, 2003).

Translation of the coronavirus polyproteins pp1a and pp1ab is coupled with extensive proteolytic processing by virus-encoded papain-like cysteine proteinases (PL1^{pro} and PL2^{pro}) and a 3C-like cysteine protease (3Cl^{pro} or main proteinase) (Ziebuhr *et al.*, 2000). The conservation of both the positions and sequences of PL1^{pro}/PL2^{pro} and 3Cl^{pro} cleavage sites allows their location in the FIPV WSU-79/1146 polyproteins to be predicted (Table 1). These predictions support the reported substrate specificity of the FIPV 3Cl^{pro} (Hegyi & Ziebuhr, 2002) and indicate that, as for other coronaviruses, there are 11 3Cl^{pro} cleavages in total in pp1a/pp1ab. With three Pl^{pro} cleavage sites in pp1a/pp1ab, this means that the replicase polyproteins can be processed into a total of 16 non-structural polypeptides (nsp1–nsp16).

Comparison of the sequences of the non-structural proteins of FIPV WSU-79/1146 with those of TGEV, HCoV-229E, MHV and IBV (Table 1) is, again, consistent with the accepted phylogeny and, as has been observed for many coronaviruses, shows that the polypeptides encoded by ORF 1b are more highly conserved than those encoded by ORF 1a. Broadly, this has been interpreted to reflect the linear organization of non-structural proteins that have essential replicative functions downstream of the 3Cl^{pro} domain, and a number of non-structural proteins that have diverged, perhaps due to host-specific adaptations, located upstream of the 3Cl^{pro} domain. It is noticeable that the FIPV WSU-79/1146 nsp1 and nsp5 polypeptides appear to have diverged less from their ancestral homologues than the other amino-proximal polypeptides of pp1a/pp1ab.

The functions associated with the FIPV WSU-79/1146 non-structural proteins can be predicted by comparison with other coronaviruses. On the basis of bioinformatic analysis, Gorbalenya and colleagues (Snijder *et al.*, 2003, 2005) have proposed enzymic activities for seven of the coronavirus non-structural proteins (nsp3, nsp5, nsp12, nsp13, nsp14, nsp15 and nsp16) and four of these (nsp3, nsp5, nsp13 and nsp15) have been confirmed by experiment (Ziebuhr, 2005).

Table 1. Predicted FIPV WSU-79/1146 replicase-cleavage products

Comparisons of predicted FIPV non-structural proteins with those of TGEV-Purdue (GenBank accession no. NC_002306), HCoV-229E (NC_002645), MHV-A59 (NC_001846) and IBV-Beaudette (NC_001451) were done by using MEGALIGN (DNASTAR, Jotun Hein method expressed as percentage amino acid identity). Protease-cleavage sites within the replicase polyprotein were predicted by alignment with the replicase polyproteins of TGEV, MHV and IBV. Abbreviations: nsp, non-structural protein; TI, translation initiation; TT, translation termination; RFS, ribosomal frameshift; PL^{pro}, papain-like proteinase; 3Cl^{pro}, 3C-like proteinase; ADRP, ADP-ribose 1″-phosphatase; ssRNA, single-strand RNA; RdRp, RNA-dependent RNA polymerase.

Cleavage product	Polyprotein	Position in polyprotein (amino acid residues)	Size (aa)	Expression	Amino acid identity (%)				Putative function(s)
					TGEV	HCoV (229E)	MHV	IBV	
nsp1	pp1a/pp1ab	1Met–Gly110	110	TI + PL^{pro}	93·6	28·2	13·6	–	
nsp2	pp1a/pp1ab	111Ala–Gly879	769	PL^{pro}	78·8	35·2	15·3	13·8	
nsp3	pp1a/pp1ab	880Gly–Gly2336	1457	PL^{pro}	79·0	34·2	18·7	14·5	PL^{pro}(s), ADRP
nsp4	pp1a/pp1ab	2337Ser–Gln2826	490	PL^{pro} + 3Cl^{pro}	87·7	50·8	30·8	24·7	
nsp5	pp1a/pp1ab	2827Ser–Gln3128	302	3Cl^{pro}	93·1	60·7	46·8	43·3	3CL^{pro}
nsp6	pp1a/pp1ab	3129Ser–Gln3422	294	3Cl^{pro}	78·2	40·6	26·8	23·6	
nsp7	pp1a/pp1ab	3423Ser–Gln3505	83	3Cl^{pro}	96·4	67·9	40·5	40·5	
nsp8	pp1a/pp1ab	3506Ser–Gln3700	195	3Cl^{pro}	92·9	61·7	42·9	42·2	
nsp9	pp1a/pp1ab	3701Asn–Gln3811	111	3Cl^{pro}	89·3	59·1	38·2	33·6	ssRNA binding
nsp10	pp1a/pp1ab	3812Ala–Gln3946	135	3Cl^{pro}	92·6	70·6	58·1	53·7	
nsp11	pp1a	3947Gly–Asp3965	19	3Cl^{pro} + TT	–	–	–	–	
nsp12	pp1ab	3947Gly–Gln4876	929	RFS + 3Cl^{pro}	97·8	74·6	59·2	59·6	RdRp
nsp13	pp1ab	4877Ala–Gln5475	599	RFS + 3Cl^{pro}	99·0	74·9	59·7	58·4	Helicase
nsp14	pp1ab	5476Ala–Gln5994	519	RFS + 3Cl^{pro}	99·0	71·6	51·8	51·5	Exonuclease
nsp15	pp1ab	5995Ser–Gln6333	339	RFS + 3Cl^{pro}	98·2	65·6	42·7	36·8	Endoribonuclease
nsp16	pp1ab	6334Ser–Pro6633	300	RFS + 3Cl^{pro} + TT	97·7	70·1	55·4	50·8	2′-O-methyltransferase

These enzymic activities are listed as putative functions of the FIPV WSU-79/1146 non-structural proteins in Table 1.

Detailed analysis of the predicted amino acid sequences of the FIPV WSU-79/1146 structural proteins reveals that they show the features characteristic of other coronavirus spike, envelope, membrane and nucleocapsid proteins. These features are listed in Supplementary Table S3, available in JGV Online. Additionally, all coronaviruses encode a number of proteins that are thought to be dispensable for replication in cell culture, but apparently provide a selective advantage *in vivo*. The genes encoding these so-called 'accessory' proteins are usually located in distinct clusters, downstream of the replicase-protein genes. In the case of FIPV WSU-79/1146, two regions of the genome that encode putative accessory proteins have been identified in previous studies (Haijema *et al.*, 2003, 2004). One is located between the S and E protein genes and one is located downstream of the N protein gene; they are known as ORFs 3abc and ORFs 7ab, respectively. Analysis of the sequence of the ORF 7ab region of the FIPV WSU-79/1146 genome reported here allows us to identify an ORF that corresponds to the previously recognized ORF 7a. It is not possible to identify an ORF that would correspond to ORF 7b. However, if a single nucleotide change were permitted (namely, if nt U_{28374} was replaced with C_{28374}), it would be possible to restore a single, large ORF that would correspond to the previously recognized ORF 7b. In the case of the ORF 3abc region, it is possible to identify ORFs that correspond to the previously recognized ORFs 3a and 3b (Haijema *et al.*, 2003). ORF 3c is not apparent. However, we note that, with two additional nucleotide insertions, it would be possible to extend ORF3b to a position that overlaps with the downstream ORF E. Further experiments will be needed to identify the translation products of both the ORF 7ab and ORF 3abc regions of the FIPV WSU-79/1146 genome, as well as for isolates that have not been propagated in cell culture for extended periods of time.

As described above, it is the TRS elements that determine the fusion sites of leader and 'body'-derived sequences of coronavirus mRNAs, and the number of TRS elements correlates with the number of subgenomic mRNAs produced by a particular virus. The TRS sequence for FIPV has been identified as containing the motif 5′-CUAAAC-3′ (de Groot *et al.*, 1988) and our sequence analysis shows that this motif occurs 11 times in the FIPV WSU-79/1146 genome. de Groot *et al.* (1987) have shown previously that at least five subgenomic mRNAs are produced in FIPV WSU-79/1146-infected cells and our analysis suggests that six are produced (Fig. 1). As has been pointed out by others (Zúñiga *et al.*, 2004), it is clear from these data that, although the TRS core motif is essential for the discontinuous
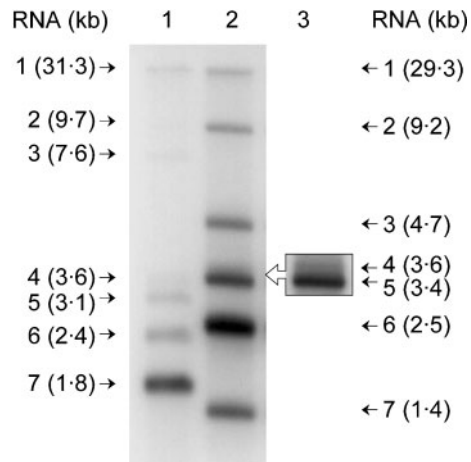
Fig. 1. Northern blot analysis of poly(A)-containing RNA from FIPV WSU-79/1146-infected CrFK cells. A ^{32}P-labelled probe was used to detect the genomic and subgenomic mRNAs of FIPV WSU-79/1146 (lane 2) or MHV A59 (lane 1). FCoV RNAs were detected by hybridization with a 986 bp, α-^{32}P random prime-labelled (Megaprime; Amersham Biosciences) PCR product corresponding to sequences in ORF 7 and the 3′ UTR of the FCoV genome. Poly(A)-containing RNA from MHV-infected cells was a kind gift from Dr H. Stokes and was detected by hybridization with a 466 bp, α-^{32}P random prime-labelled PCR product corresponding to sequences in the N protein ORF of the MHV genome. The sizes of the RNAs are indicated in kb. Lane 3 contains the same material as lane 2, electrophoresed on a 1·3 % agarose gel to increase resolution in the region of mRNAs 4 and 5.

Fig. 2. Alignment of FIPV WSU-79/1146 TRS elements. Nucleotides matching the leader TRS are underlined. These sequences represent the leader–body junctions of the subgenomic mRNAs. The minimal consensus sequence, or 'core motif' of the TRS, that is present in all functional TRS elements is shaded. The initiation codons for the mRNA translation product(s) are shown in bold.

extension of coronavirus ($-$)-strand templates, it is not sufficient.

The final analysis that we undertook in this study was to determine the sequence of the TRS–body 'junctions' for each of the intracellular mRNAs of FIPV WSU-79/1146. To do this, the 5′-proximal regions of mRNAs 2–7 were amplified by RT-PCR and sequenced. The conclusions are summarized in Fig. 2. The analysis confirms the minimal TRS core sequence of FIPV WSU-79/1146 as 5′-CUAAAC-3′. The fact that the abundance of the subgenomic mRNAs does not correlate with the potential for base pairing between the leader and complement of the body TRS elements indicates, again, that additional factors (e.g. proteins) must be involved in the process of discontinuous extension that takes place during synthesis of the subgenomic ($-$)-strand templates.

This study provides the first comprehensive analysis of the FIPV WSU-79/1146 genome sequence, including a complete consensus sequence for the non-structural protein-coding region of the genome. Thus, it is now possible to predict the primary sequence of the full complement of FCoV non-structural proteins and oligonucleotide primers can be designed for the cloning and expression of each of these genes. The availability of recombinant forms of the FIPV WSU-79/1146 non-structural proteins will help to provide a more detailed understanding of their structure and function. Secondly, this study predicts a number of *cis*-acting RNA elements in the genome that may be involved in FCoV replication and transcription. Directed mutagenesis and structural methods can now be used to investigate the structure–function relationships of these elements. Thirdly, the genomic sequence of FIPV WSU-79/1146 can now be compared with the sequence of RNA from clinical isolates or RNA amplified from clinical material. This sort of information will have, for example, important implications for development of prophylactic or therapeutic strategies to control or prevent FCoV infections.

Acknowledgements

References

Addie, D. D. (2000). Clustering of feline coronaviruses in multicat households. *Vet J* **159**, 8–9.

Addie, D. D. & Jarrett, J. O. (1992). Feline coronavirus antibodies in cats. *Vet Rec* **131**, 202–203.

Addie, D. D. & Jarrett, O. (2001). Use of a reverse-transcriptase polymerase chain reaction for monitoring the shedding of feline coronavirus by healthy cats. *Vet Rec* **148**, 649–653.

Brierley, I. (1995). Ribosomal frameshifting on viral RNAs. *J Gen Virol* **76**, 1885–1892.

de Groot, R. J., ter Haar, R. J., Horzinek, M. C. & van der Zeijst, B. A. M. (1987). Intracellular RNAs of the feline infectious peritonitis coronavirus strain 79-1146. *J Gen Virol* **68**, 995–1002.

de Groot, R. J., Andeweg, A. C., Horzinek, M. C. & Spaan, W. J. M. (1988). Sequence analysis of the 3′ end of the feline coronavirus FIPV 79-1146 genome: comparison with the genome of porcine coronavirus TGEV reveals large insertions. *Virology* **167**, 370–376.

Goebel, S. J., Hsue, B., Dombrowski, T. F. & Masters, P. S. (2004). Characterization of the RNA components of a putative molecular

switch in the 3′ untranslated region of the murine coronavirus genome. *J Virol* **78**, 669–682.

González, J. M., Gomez-Puertas, P., Cavanagh, D., Gorbalenya, A. E. & Enjuanes, L. (2003). A comparative sequence analysis to revise the current taxonomy of the family *Coronaviridae*. *Arch Virol* **148**, 2207–2235.

Gosert, R., Kanjanahaluethai, A., Egger, D., Bienz, K. & Baker, S. C. (2002). RNA replication of mouse hepatitis virus takes place at double-membrane vesicles. *J Virol* **76**, 3697–3708.

Haijema, B. J., Volders, H. & Rottier, P. J. M. (2003). Switching species tropism: an effective way to manipulate the feline coronavirus genome. *J Virol* **77**, 4528–4538.

Haijema, B. J., Volders, H. & Rottier, P. J. M. (2004). Live, attenuated coronavirus vaccines through the directed deletion of group-specific genes provide protection against feline infectious peritonitis. *J Virol* **78**, 3863–3871.

Hegyi, A. & Ziebuhr, J. (2002). Conservation of substrate specificities among coronavirus main proteases. *J Gen Virol* **83**, 595–599.

Herrewegh, A. A. P. M., Smeenk, I., Horzinek, M. C., Rottier, P. J. M. & de Groot, R. J. (1998). Feline coronavirus type II strains 79-1683 and 79-1146 originate from a double recombination between feline coronavirus type I and canine coronavirus. *J Virol* **72**, 4508–4514.

Pedersen, N. C. (1995). An overview of feline enteric coronavirus and infectious peritonitis virus infections. *Feline Pract* **23**, 7–20.

Poland, A. M., Vennema, H., Foley, J. E. & Pedersen, N. C. (1996). Two related strains of feline infectious peritonitis virus isolated from immunocompromised cats infected with a feline enteric coronavirus. *J Clin Microbiol* **34**, 3180–3184.

Prentice, E., Jerome, W. G., Yoshimori, T., Mizushima, N. & Denison, M. R. (2004). Coronavirus replication complex formation utilizes components of cellular autophagy. *J Biol Chem* **279**, 10136–10141.

Raman, S., Bouma, P., Williams, G. D. & Brian, D. A. (2003). Stem-loop III in the 5′ untranslated region is a *cis*-acting element in bovine coronavirus defective interfering RNA replication. *J Virol* **77**, 6720–6730.

Sawicki, S. G. & Sawicki, D. L. (1990). Coronavirus transcription: subgenomic mouse hepatitis virus replicative intermediates function in RNA synthesis. *J Virol* **64**, 1050–1056.

Siddell, S. G., Ziebuhr, J. & Snijder, E. J. (2005). Coronaviruses, toroviruses and arteriviruses. In *Topley and Wilson's Microbiology and Microbial Infections*, 10th edn. Edited by B. W. J. Mahy & V. ter Meulen. London: Edward Arnold (in press).

Snijder, E. J., Bredenbeek, P. J., Dobbe, J. C. & 7 other authors (2003). Unique and conserved features of genome and proteome of SARS-coronavirus, an early split-off from the coronavirus group 2 lineage. *J Mol Biol* **331**, 991–1004.

Snijder, E. J., Siddell, S. G. & Gorbalenya, A. E. (2005). The order Nidovirales. In *Topley and Wilson's Microbiology and Microbial Infections*, 10th edn. Edited by B. W. J. Mahy & V. ter Meulen. London: Edward Arnold (in press).

Spaan, W., Delius, H., Skinner, M., Armstrong, J., Rottier, P., Smeekens, S., van der Zeijst, B. A. & Siddell, S. G. (1983). Coronavirus mRNA synthesis involves fusion of non-contiguous sequences. *EMBO J* **2**, 1839–1844.

Sparkes, A. H., Gruffydd-Jones, T. J. & Harbour, D. A. (1992). Feline coronavirus antibodies in UK cats. *Vet Rec* **131**, 223–224.

Thiel, V., Rashtchian, A., Herold, J., Schuster, D. M., Guan, N. & Siddell, S. G. (1997). Effective amplification of 20-kb DNA by reverse transcription PCR. *Anal Biochem* **252**, 62–70.

Thiel, V., Ivanov, K. A., Putics, Á. & 9 other authors (2003). Mechanisms and enzymes involved in SARS coronavirus genome expression. *J Gen Virol* **84**, 2305–2315.

Van Den Born, E., Gultyaev, A. P. & Snijder, E. J. (2004). Secondary structure and function of the 5′-proximal region of the equine arteritis virus RNA genome. *RNA* **10**, 424–437.

Vennema, H., Poland, A., Foley, J. & Pedersen, N. C. (1998). Feline infectious peritonitis viruses arise by mutation from endemic feline enteric coronaviruses. *Virology* **243**, 150–157.

Watt, N. J., MacIntyre, N. J. & McOrist, S. (1993). An extended outbreak of infectious peritonitis in a closed colony of European wildcats (*Felis silvestris*). *J Comp Pathol* **108**, 73–79.

Ziebuhr, J. (2005). The coronavirus replicase. *Curr Top Microbiol Immunol* **287**, 57–94.

Ziebuhr, J., Snijder, E. J. & Gorbalenya, A. E. (2000). Virus-encoded proteinases and proteolytic processing in the *Nidovirales*. *J Gen Virol* **81**, 853–879.

Zúñiga, S., Sola, I., Alonso, S. & Enjuanes, L. (2004). Sequence motifs involved in the regulation of discontinuous coronavirus subgenomic RNA synthesis. *J Virol* **78**, 980–994.